

## ANALYZING EXTREME SEA STATE CONDITIONS BY TIME-SERIES SIMULATION

Erik Vanem

DNV GL Group Technology & Research, Høvik, Norway  
Department of Mathematics, University of Oslo, Oslo, Norway

### ABSTRACT

*This paper presents an extreme value analysis on data of significant wave height based on time-series simulation. A method to simulate time series with given marginal distribution and preserving the autocorrelation structure in the data is applied to significant wave height data. Then, extreme value analysis is performed by simulating from the fitted time-series model that preserves both the marginal probability distribution and the autocorrelation. In this way, the effect of serial correlation on the extreme values can be taken into account, without subsampling and de-clustering of the data. The effect of serial correlation on estimating extreme wave conditions have previously been highlighted, and failure to account for this effect will typically lead to an overestimation of extreme conditions. This is demonstrated by this study, that compares extreme value estimates from the simulated times-series model with estimates obtained directly from the marginal distribution assuming that 3-hourly significant wave heights are independent and identically distributed. A dataset of significant wave height provided as part of a second benchmark exercise on environmental extremes that was presented at OMAE 2021, has been analysed.*

Keywords: Ocean environment; Extreme value analysis; Time series modelling; Significant wave height; Environmental loads; probabilistic wave models

### 1 INTRODUCTION

Probabilistic descriptions of extreme wave conditions are important for safe and reliable design and operation of marine structures. The most extreme environmental conditions the structure is expected to experience during its lifetime must be ac-

counted for during design, and extreme value analysis of relevant metocean variables is crucial. One of the most relevant wave parameters for ocean engineering applications is the significant wave height,  $H_S$ , and several applications of extreme value analysis of this variable has been reported in the literature [1–8]. Indeed, a second benchmark exercise was announced at OMAE 2021 calling for estimates of extreme environmental conditions based on specific datasets of significant wave height that were made available [9]. This is a follow-up of a previous benchmarking exercise that, inter alia, highlighted the effect of serial correlation on extreme value estimates [10], as elaborated further in [11].

This paper presents extreme value estimates of significant wave height from the datasets presented in the second benchmark exercise, based on a time-series model that preserves the marginal distribution and the autocorrelation of the data. This is a way of accounting for serial correlation in the statistical analysis that would reduce the bias this has on extreme value estimates, but without the need for subsampling and de-clustering of the data. Such modelling could also provide a means for more realistic simulation of time-series of significant wave height that could be relevant for other applications than extreme value analysis, even though the focus of this paper is estimation of extreme conditions.

The extreme value analysis presented in this paper is based on simulating time-series from the fitted statistical model to obtain several samples of the extreme  $T$ -year significant wave height. This gives an empirical distribution of the maximum  $H_S$  in a  $T$ -year period, and the corresponding  $T$ -year return value can be estimated as the  $1/e$ -quantile of this distribution (see e.g. [9, 11]). However, the approach presented in this paper gives

an estimate of the full  $T$ -year maximum distribution and other measures such as the mean and standard deviation of the  $T$ -year maximum can also be estimated. Moreover, a parametric distribution may be fitted to the empirical extreme value distribution. In this paper, the focus will be on the 25-year extreme values.

In the following, a brief description of the significant wave height data used in this study will be given before the statistical model will be presented. Finally, results from applying such a model to the significant wave height data will be presented and discussed.

## 2 SIGNIFICANT WAVE HEIGHT DATA

Three different datasets of significant wave height, referred to as Site 1, Site 2 and Site 3, respectively, have been made available as part of the second benchmark exercise [9]. In all datasets, values of significant wave height at 3-hourly intervals are provided for a period of 25 years. Trace plots of the data for the three sites are shown in Figure 1, where the index on the x-axis denotes the 3-hourly intervals, and the empirical densities are shown in Figure 2. Some summary statistics of the data are provided in Table 1. The 25-year return value estimates presented in this table are from a standard block-maxima approach on annual maximum data assuming a generalized extreme value distribution, see e.g. [12], and are provided for reference. It is noted that these estimates are somewhat different from the baseline estimates provided in [9], which were based on the block maximum approach on annual maxima but assuming a Gumbel distribution. These differences only illustrates the large uncertainties associated with extreme value analysis. Note also that although the most severe conditions in the baseline results presented in [9] are associated with Site 1, the summary statistics in Table 1 suggest that the most severe conditions occur at Site 3. Hence, it is possible that the naming of the datasets have been mixed up and that what is referred to as Site 1 in [9] is indeed dataset Site 3 in this paper. However, as long as one do not intend to compare results, the naming of the datasets has no relevance. Note also that all datasets have positive skewness, indicating right-skewed distributions, and that the kurtoses are greater than 3, indicating heavier tails than the normal distribution.

## 3 STATISTICAL MODEL FOR TIME-SERIES SIMULATION

Typically, in extreme value analysis, one may fit statistical models to the peaks in the data only, e.g. model peaks over a threshold or block maxima, which may be assumed to be independent and identically distributed (iid) after sensible de-clustering. In this way, serial correlations are removed in the data that are analysed, and the effect of serial correlation will be negligible. However, one drawback of this approach is that it is wasteful, and the amount of data available for the analysis is

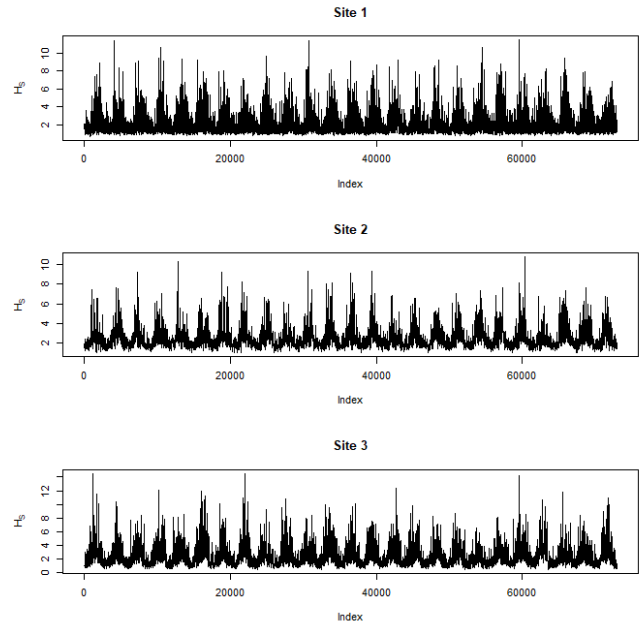


FIGURE 1. Trace plots of the significant wave height data

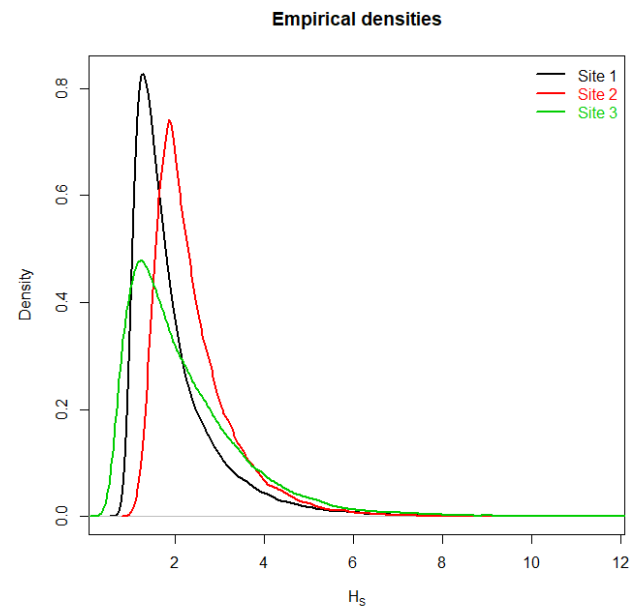


FIGURE 2. Empirical densities of the significant wave height data

significantly reduced. Typically, with an annual maximum approach, the amount of data is reduced to 25 from 25 years of observations. Even though the bias due to serial correlation is avoided, the uncertainty due to sampling variability will be rather

**TABLE 1.** Summary statistics for the significant wave height data (in meters).

	Site 1	Site 2	Site 3
minimum	0.72	1.01	0.41
median	1.64	2.16	1.85
mean	1.95	2.41	2.20
90%tile	3.19	3.58	3.91
99%tile	5.85	5.60	6.87
maximum	11.44	10.79	14.53
standard deviation	1.01	0.90	1.32
skewness	2.38	1.78	1.81
kurtosis	11.42	7.79	8.35
25-year return value	11.36	11.33	14.34
50-year return value	11.78	12.93	15.16

large.

In this paper, a different approach is suggested that explicitly takes the serial correlation into account in the statistical modelling. That is, rather than merely fitting a distribution function to the data and making inference based on that, a statistical model that both preserves the marginal distribution and the autocorrelation in the data will be established, and estimates of extreme values will be based on that model. There are different approaches that could be used in order to establish such time-series models [13]. For example, [14, 15] propose diffusion-type models with given marginal distributions and autocorrelation functions, Weibull and gamma autoregressive processes are presented in [16], and Gaussian and Non-Gaussian autoregressive models are discussed in [17]. However, in this paper, an approach based on transforming a Gaussian parent autoregressive time series to have the desired marginal distribution and temporal correlation structure will be taken, as suggested in [18]; see also [19, 20].

The time-series of interest,  $X(t)$ , is specified by a marginal distribution,  $F_X(x)$  and an autocorrelation structure,  $\rho_X(\tau)$  and it is assumed that this has a parent Gaussian time-series,  $Z(t)$  with a standard Gaussian marginal  $\Phi_Z(z)$  and another autocorrelation structure  $\rho_Z(\tau)$ . Hence, modelling and simulation of the time-series  $X(t)$  correspond to modelling and simulating the parent Gaussian time-series and finding the transformations that transform the parent time-series to the desired one, i.e. determine functions  $g$  and  $\mathcal{T}$  such that

$$\begin{aligned} X(t) &= g(Z(t)) \\ \rho_Z(\tau) &= \mathcal{T}(\rho_X(\tau)) \end{aligned} \quad (1)$$

Simulating from a Gaussian time-series is not difficult, and the normal distribution have several well-know properties. For example, if  $Z(t)$  is a standard normal time-series, then any linear combination of  $Z(t)$ 's will be jointly normally distributed and the

marginal will be standard normal. Hence, if one can find a parent Gaussian time-series that can be transformed into the time-series  $X(t)$ , simulation of  $X(t)$  is straightforward.

As pointed out in [18],  $g$  is easily identified as  $g(Z) = F_X^{-1}(\Phi_Z(Z))$ , which will give the desired marginal distribution. However, this transformation of the marginal distribution does not preserve the autocorrelation structure, which depends on the marginal distribution  $F_X(x)$ . Hence, one needs to establish the autocorrelation structure of the parent Gaussian time-series,  $\rho_Z(\tau)$  that yields the required autocorrelation structure for the target time-series  $X(t)$  after transformation.

In the bivariate case, it can be shown that for an arbitrary transformation, the correlation between the transformed variables will be smaller than the correlation between the initial standard normal variables (see e.g. [18]), i.e.

$$\rho_X = \text{Cor}[g(Z(t_1)), g(Z(t_2))] \leq \text{Cor}[Z(t_1), Z(t_2)] = \rho_Z, \quad (2)$$

meaning that the  $\rho_Z$  values needs to be inflated to obtain the target  $\rho_X$ . Moreover, the correlation coefficient of two lagged variables  $X(t_1)$  and  $X(t_2)$  can be expressed as

$$\rho_X(\tau) = \frac{E(X(t_1)X(t_2)) - \mu_X^2}{\sigma_X^2}, \quad (3)$$

where  $E$  is the expectation operator,  $\tau = t_2 - t_1$  and  $\mu_X$  and  $\sigma_X$  are the mean and the standard deviation of  $X$ . Now, assuming that  $X(t) = g(Z(t)) = F_X^{-1}(\Phi_Z(Z(t)))$ , one has that

$$\begin{aligned} E(X(t_1)X(t_2)) &= E(F_X^{-1}(\Phi_Z(Z(t_1)))F_X^{-1}(\Phi_Z(Z(t_2)))) \\ &= \int_{-\infty}^{\infty} \int_{-\infty}^{\infty} F_X^{-1}(\Phi_Z(u))F_X^{-1}(\Phi_Z(v))\phi_{u,v}(u,v;\rho_Z(t_2-t_1))dudv, \end{aligned} \quad (4)$$

where  $\phi(u,v;\rho)$  denotes the density function of the bivariate standard normal distribution with correlation  $\rho$ . This gives a relationship between  $\rho_Z(\tau)$  and  $\rho_X(\tau)$  and can be used to calculate  $\rho_X(\tau)$  from known  $\rho_Z(\tau)$ , i.e.

$$\rho_X(\tau) = \frac{\int_{-\infty}^{\infty} \int_{-\infty}^{\infty} F_X^{-1}(\Phi_Z(u))F_X^{-1}(\Phi_Z(v))\phi_{u,v}(u,v;\rho_Z(\tau))dudv - \mu_X^2}{\sigma_X^2}. \quad (5)$$

Note however, that in order to model the time series with known  $\rho_X(t)$ , one needs the inverse transformation to find  $\rho_Z(t)$  from  $\rho_X(t)$ . Note also that even though the double integral above does

not have an analytical solution in general, its numerical estimation is straightforward.

Hence, the modelling problem is solved by defining a correlation transformation function to estimate the autocorrelation of the parent Gaussian time-series from a given target autocorrelation structure that may be estimated from the data. The following parametric form of such an autocorrelation transformation function is proposed in [18]:

$$\rho_Z = \mathcal{T}(\rho_X) = \frac{(1 + \alpha\rho_X)^{(1-\beta)} - 1}{(1 + \alpha)^{(1-\beta)} - 1}. \quad (6)$$

This can be used to estimate a parametric autocorrelation function of the parent Gaussian time-series,  $\rho_Z(\tau)$  based on a parametric autocorrelation function for the target time-series,  $\rho_X(\tau)$ . The parameters can be fitted by calculating  $\rho_X$  for  $\rho_Z = (0.1, 0.2, 0.3, 0.4, 0.5, 0.6, 0.7, 0.8, 0.9, 0.95)$  according to eq. (5) and fit the function to the set of  $(\rho_X, \rho_Z)$ -points (see [18] for details).

With this approach, modelling a time series with desired marginal and correlation structure involves fitting the marginal distribution and estimating the empirical autocorrelation structure from the time-series, fitting the parametric autocorrelation transformation function to obtain the autocorrelation structure of the parent Gaussian time-series, fit an autoregressive model to generate the Gaussian parent time-series and transforming the Gaussian time-series using the transformation  $X(t) = g(Z(t)) = F_X^{-1}(\Phi(Z(t)))$ . In the following, such a model will be fitted to the three datasets of significant wave height by estimating the marginal distributions and the autocorrelation functions.

### 3.1 Marginal distributions

The first step in the modelling approach presented above is to fit a marginal distribution to the data. For significant wave height data, the 3-parameter Weibull distribution is often assumed to give a good fit [21], and this distribution will be assumed also in this study. Hence, the 3-parameter Weibull distribution, with density function given in Eq. (7), will be fitted to the three datasets. Two fitting techniques will be tried, i.e. maximum likelihood (ML) and fitting based on the second order Anderson-Darling statistic (AD), see e.g. [22]. The resulting fits are shown in Figure 3, and estimated model parameters are shown in Table 2. It is observed that the marginal fits are not too good, but AD-fits are considerably better for the upper tail compared to the ML-fits, although completely missing the lower values, and these marginal distributions will be assumed in the further analysis.

$$f_{H_s}(h_s) = \frac{\beta}{\alpha} \left( \frac{h_s - \gamma}{\alpha} \right)^{\beta-1} \exp \left[ - \left( \frac{h_s - \gamma}{\alpha} \right)^{\beta} \right]. \quad (7)$$

It is noted that improved fits could possibly be obtained by using other fitting methods, e.g. the method of moments, or by assuming other parametric distribution functions, for example a hybrid model with a Weibull distribution for the body and a generalized Pareto distribution for the tails. However, for the purpose of this study, the 3-parameter Weibull distribution fitted by minimizing the second order Anderson-Darling statistic will be assumed, and this is found to capture the upper tail quite well.

**TABLE 2.** Fitted model parameters for the marginal distributions.

		shape ( $\beta$ )	Scale ( $\alpha$ )	location ( $\gamma$ )
Site 1	ML fit	1.386	1.363	0.720
	AD fit	<b>0.873</b>	<b>0.817</b>	<b>1.085</b>
Site 2	ML fit	1.688	1.576	1.010
	AD fit	<b>1.049</b>	<b>0.948</b>	<b>1.488</b>
Site 3	ML fit	1.472	1.996	0.410
	AD fit	<b>1.058</b>	<b>1.419</b>	<b>0.828</b>

The parametric function assumed for the autocorrelation transformation function in eq. (6) is found to fit the autocorrelation transformation points very well, as demonstrated in Figure 4 for the three marginal distributions fitted to the different datasets in this study.

### 3.2 Autocorrelation functions

In order to specify the autocorrelation of the parent Gaussian autoregressive model, one must estimate the autocorrelation function for the target time-series, and this is done by fitting a parametric function to the empirical autocorrelation function (ACF). There are many parametric autocorrelation functions to choose from, see e.g. [18] and in this study, six different parametric functions is tried out, i.e. the Weibull, the Burr, the logarithmic, the fGn, the generalised fGn and the Pareto ACF. The empirical autocorrelation functions are shown together with the fitted parametric candidate models in Figure 5. The functions are fitted by least squares, and the residual sum of squares (RSS) are indicated for each candidate model in the plots. It is observed that the 3-parameter Burr-type autocorrelation function fits best to the data for all three sites, and this would typically be preferred. However, it turns out that this ACF yields not positive definite covariance matrices (see also [23]), and therefore further analyses will be based on the 2-parameter alternatives, Weibull, logarithmic and Pareto-type ACFs. The parametric forms of these autocorrelation functions are given in Eq. (8).

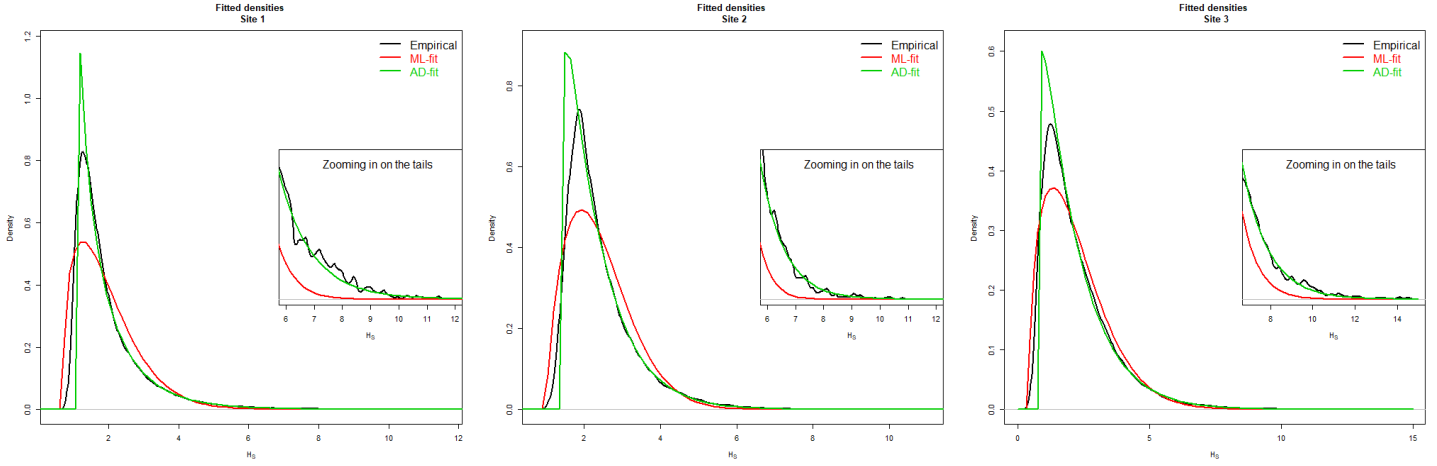


FIGURE 3. Fitted marginal distributions

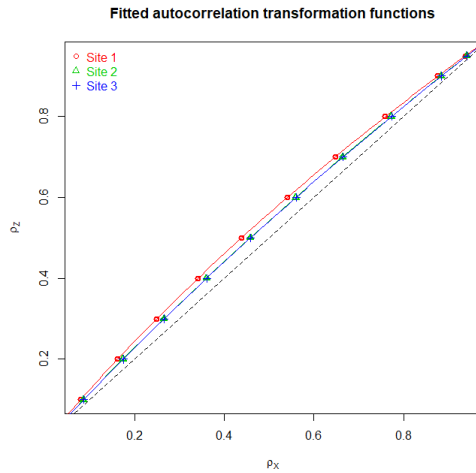


FIGURE 4. Fitted autocorrelation transformation function according to eq. (6)

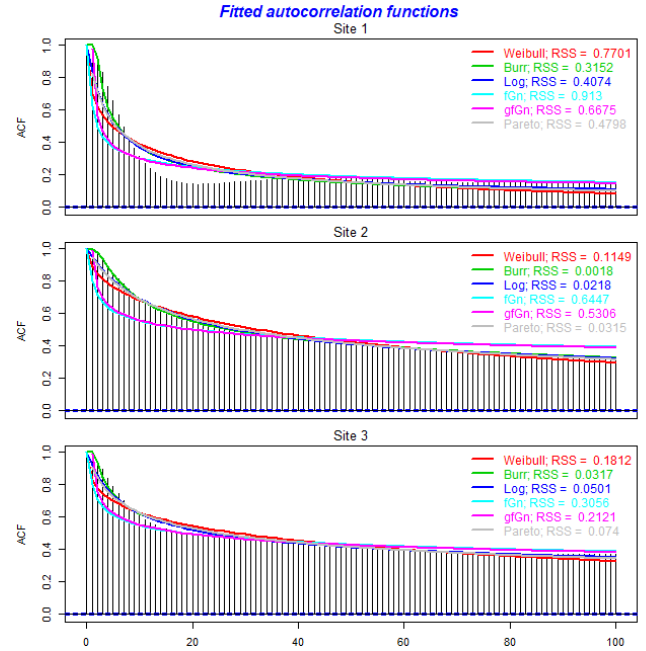
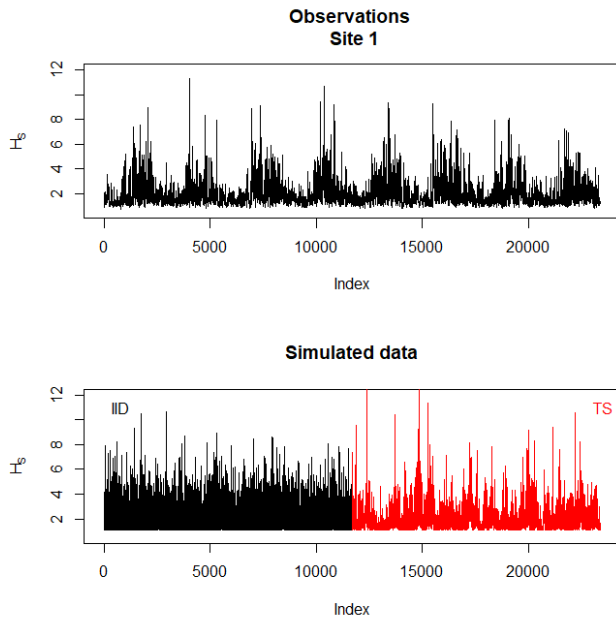


FIGURE 5. Autocorrelation functions

$$\begin{aligned}
 \rho_{Burr}(\tau; \zeta, \eta, \theta) &= \left(1 + \theta \left(\frac{\tau}{\zeta}\right)^\eta\right)^{-\frac{1}{\eta\theta}} \\
 \rho_{Weibull}(\tau; \zeta, \eta) &= e^{-\left(\frac{\tau}{\zeta}\right)^\eta} \\
 \rho_{Log}(\tau; \zeta, \eta) &= \left(1 + \ln\left(1 + \eta \frac{\tau}{\zeta}\right)\right)^{-\frac{1}{\eta}} \\
 \rho_{Pareto}(\tau; \zeta, \eta) &= \left(1 + \eta \frac{\tau}{\zeta}\right)^{-\frac{1}{\eta}}
 \end{aligned} \tag{8}$$

Having established the statistical model, it is possible to sim-

ulate from it to generate simulated data with the desired marginal distribution and autocorrelation function. Examples of such simulated data are shown in Figure 6. The top plot shows 8 years of observed data from Site 1 and the bottom plot shows first 4 years of data simulated from the fitted marginal distribution assuming iid and then four years of data simulated from the time-series model assuming the same marginal distribution and a Weibull-type autocorrelation function. It is observed that the data simulated from the time-series model better resemble the observed data than the data simulated assuming iid.



**FIGURE 6.** Comparing observed (top) and simulated (bottom) data; simulated data are from the marginal distribution assuming iid and from the time-series model with desired marginal and autocorrelation function, respectively

#### 4 EXTREME VALUE ANALYSIS RESULTS

Having established the statistical models, it is possible to simulate synthetic time series of significant wave height for the three sites in order to do extreme value analysis. In this study,  $M = 500$  25-year time series will be simulated from the statistical models. For each simulated time-series the largest value is taken to represent a sample of the 25-year maximum significant wave height. This yields  $M = 500$  samples from the distribution and can be used to make inference of the 25-year maximum significant wave height. One may estimate the entire distribution as well as for example the mean 25-year maximum significant wave height and the 25-year return value of significant wave height.

The simulated distributions of 25-year maximum significant wave height are shown in Figure 7. Results are shown for time-series models assuming the parametric Weibull, Logarithmic and Pareto autocorrelation functions, as well as for a model using the non-parametric empirical autocorrelation function. In addition, results are shown for data simulated assuming iid from the marginal distributions. The plots also include the corresponding estimates of the 25-year return values for significant wave height, as well as the quantile of the marginal distribution corresponding to the 25-year return value if serial correlation is ignored.

Some general observations can be made from these results. Firstly, it is observed that the assumed autocorrelation function notably influences the return value estimates. For all of the

sites, assuming the same marginal distribution, return value estimates vary according to what parametric autocorrelation function was fitted to the data. For all the sites, the ordering of return value estimates according to which autocorrelation function is assumed remains the same. Simply using the empirical non-parametric autocorrelation function to fit the time series model yields the lowest return value estimate. Then, increasing estimates are obtained by assuming, the logarithmic, the Pareto-type and the Weibull-type parametric acfs, respectively. It is not obvious whether this is a particular feature of these datasets or if this is a general feature of the acfs, but it is interesting to observe that the ordering of return value estimates correspond to the ordering of model fit of the different acf, as seen from Figure 5. Hence, it seems to be the case that a better fit of the parametric acf to the empirical one yields better agreement between results assuming the empirical acf which in this case means lower return value estimates. Furthermore, it is observed that all estimates obtained from a time-series model are significantly lower than the return value estimates obtained from assuming iid and hence ignoring serial correlation. Hence, even though the best time series model cannot be determined, it seems clear that accounting for serial dependence in some way reduces or even eliminates the positive bias in return value estimates obtained when neglecting serial correlation.

For the three sites, the largest differences in the return value estimates are between estimates based on time series models with the empirical autocorrelation function and the estimates ignoring serial correlation. For site 1, the difference is 1.42 m, for site 2 it is 1.31 m and for site 3 it is 1.93 m, for the 25-year return value. This may be practically significant, suggesting that serial correlations should be taken into account in extreme value analysis for ocean engineering applications.

Results may also be compared to the reference values in Table 1 obtained from rather standard GEV-fitting to annual maxima, and it is observed that there are no recognizable patterns. For Site 1, the return value estimates obtained from fitting GEV to annual maxima are considerably lower than all estimates obtained using the time series models, and also obviously much lower than the return values obtained when ignoring serial correlation. For Site 2, the picture is completely opposite, and annual-maxima based return value estimates are considerably higher than estimates from either the time series models or from the models ignoring serial dependence. Finally, for Site 3, the annual-maxima based return value estimates fall between the estimates obtained from the time series models and the estimates obtained when ignoring time-series models. If nothing else, these observations serve to remind about the large uncertainties associated with extreme value analysis [22].

It is also possible to fit parametric distributions to the simulated  $T$ -year extreme data, and the Gumbel distribution can be assumed as a reasonable extreme value model. Hence, the resulted parametric distributions fitted to the 25-year maximum

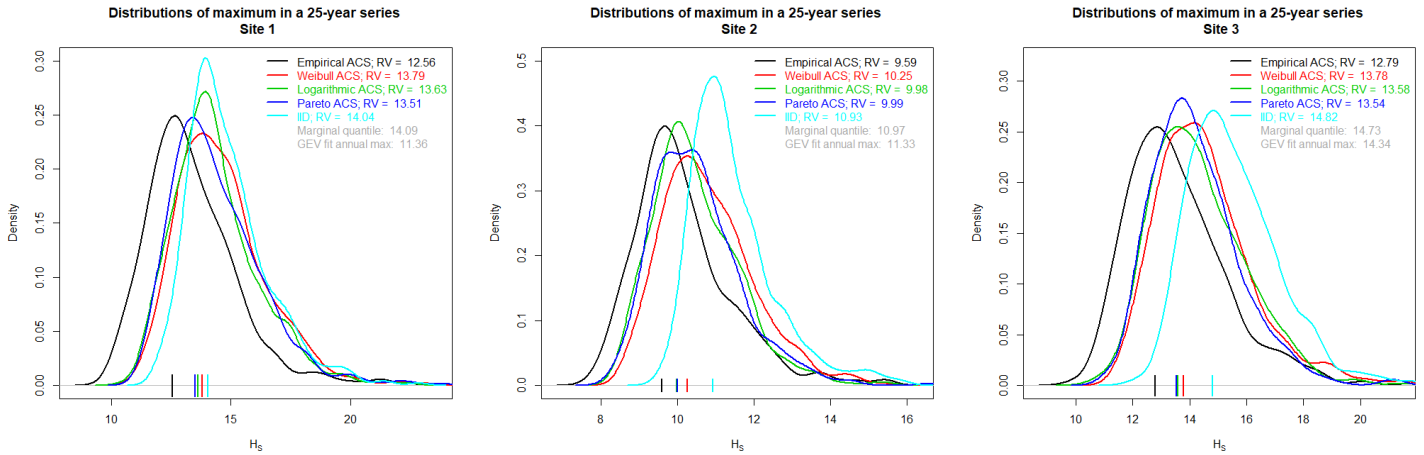


**FIGURE 7.** Distributions of 25-year maximum significant wave height from the time-series models

data for Site 1 is shown in Figure 8. The empirical distributions are shown with dashed lines and the solid lines are the fitted gumbel distributions. The fits are good and slightly different return value estimates can also be obtained from these parametric distributions, as indicated in the figure.

## 5 DISCUSSION

The extreme value analysis presented above is a way of accounting for serial correlation by simulating from a time series model that preserves the marginal distribution and the autocorrelation in the observed data. It is demonstrated to give lower extreme value estimates than what one would get if serial correlation is ignored and hence to reduce the positive bias known to occur [11]. It also has an advantage compared to standard extreme value analysis techniques in that there is no need for sub-sampling and de-clustering, making it less wasteful. However, results will be sensitive to the actual time-series model fitted to the data, in terms of both the marginal and the autocorrelation function. Indeed, different autocorrelation functions were used in this study and were found to give different results. Hence, efforts should be made to improve the time series models.

In this study, rather crude models were fitted to the data, and significant improvements could be made by for example pre-processing of the data. The autocorrelation functions were fitted directly to the observed data, and improved models could be obtained by e.g. removing any deterministic components from the time series before fitting a model to the residuals. Seasonality is one example of such deterministic components; long-term trends is another. Different ways of modelling and removing seasonal components are suggested in e.g. [24, 25]. Another approach could be to bin the data into different seasons and fit season-specific models to each bin, similarly to the approach taken by [7, 26]. Such pre-processing or binning of the data have not been explored in this study, and it is suggested as an important direction for future research.

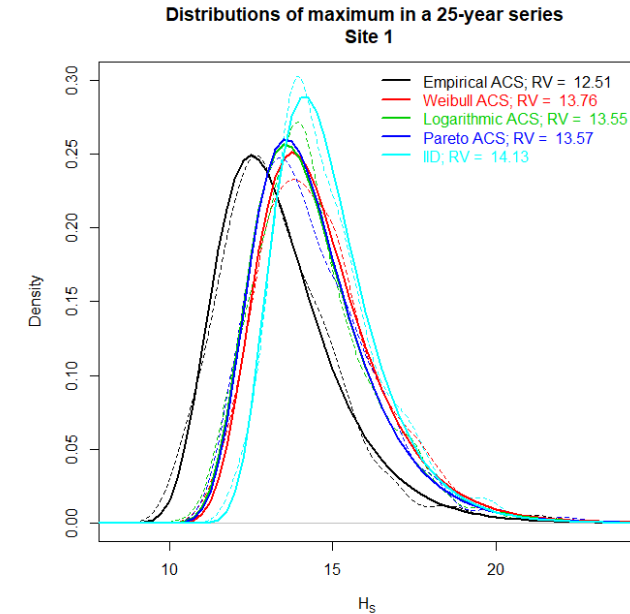


**FIGURE 8.** Fitting Gumbel distributions for the 25-year maximum data

$Pr(X(t + \tau) > u | X(t) > u)$ , which may be illustrated by extremograms [27, 28]. The correlation structure for high levels,  $u$ , should also be preserved in the time series to ensure the effect of serial correlation on extremes are properly accounted for. It is possible to compare the sample extremogram of the data and the simulated time-series, as shown in Figure 9 with levels corresponding to quantiles  $q = 0.99, 0.999$  and  $0.9995$ . As can be seen from these plots, the simulated time series preserves the extremal correlation reasonably well, and much better than the simulated IID samples (where also the extremes will be independent). The TS-extremograms shown in Figure 9 correspond to the time series simulated with the non-parametric empirical autocorrelation structure.

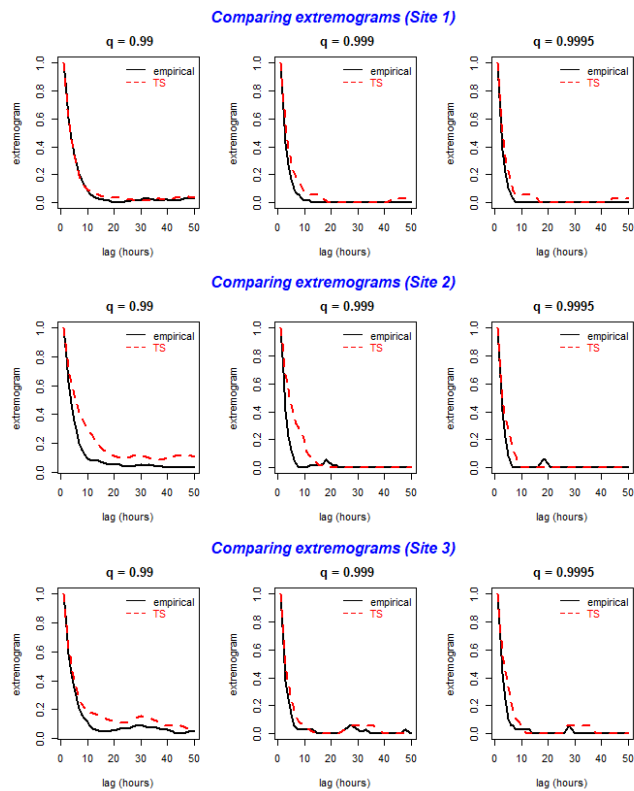


**FIGURE 9.** Comparing extremograms for the empirical data and simulated time series

## 6 SUMMARY AND CONCLUSIONS

This paper has presented an approach to fitting statistical models to metocean data that preserves the marginal distribution and the autocorrelation in the observed time series. Such models may be established from fitted marginal distributions and ei-

ther the empirical autocorrelation function or a parametric function fitted to this. These models can then be used for extreme value analysis by simulating from the fitted models in order to obtain distributions of  $T$ -year maximum data. Return values can then be estimated from these distributions, which then takes serial correlation into account. It is also demonstrated that this reduces or eliminates the positive bias that is known to occur in extreme value analysis when ignoring the effect of serial correlation. Hence, the presented approach is presented as an alternative to standard extreme value analysis approaches based on peak values, and one advantage with the proposed method is that it is not wasteful. There is no need for de-clustering or peak picking of the data. Moreover, such statistical models may have other uses than extreme value analysis.

Extreme value estimates based on the proposed approach are found to be reasonable. In particular, estimates are lower than estimates obtained when ignoring serial correlation. However, results also demonstrate that return value estimates will be sensitive to the assumed time series model. In particular, different assumptions of the autocorrelation function will give different results. Hence, particular focus should be put on obtaining the best possible model, and objective model selection criteria will be important. Furthermore, careful pre-processing of the data to remove any deterministic components should be carried out, although this has been left for future work in this study.

## Acknowledgement

The work presented in this paper has been partly carried out within the research project HIPERWIND, with support from EU H2020 (grant agreement number 101006689), and has also been supported by the center for research-based innovation, Big Insight, with support from the Research Council of Norway (grant number 237718).

## References

- [1] Muir, L. R., and El-Shaarawi, A., 1986. "On the calculation of extreme wave heights: A review". *Ocean Engineering*, **13**, pp. 93–118.
- [2] Jonathan, P., and Ewans, K., 2013. "Statistical modelling of extreme ocean environments for marine design: a review". *Ocean Engineering*, **62**, pp. 91–109.
- [3] Vanem, E., 2011. "Long-term time-dependent stochastic modelling of extreme waves". *Stochastic Environmental Research and Risk Assessment*, **25**, pp. 185–209.
- [4] Stefanakos, C. N., and Athanassoulis, G. A., 2006. "Extreme value predictions based on nonstationary time series of wave data". *Environmetrics*, **17**, pp. 25–46.
- [5] Baxevani, A., Caires, S., and Rychlik, I., 2009. "Spatio-temporal statistical modelling of significant wave height". *Environmetrics*, **20**, pp. 14–31.



- [6] Vanem, E., Huseby, A. B., and Natvig, B., 2012. “A Bayesian hierarchical spatio-temporal model for significant wave height in the North Atlantic”. *Stochastic Environmental Research and Risk Assessment*, **26**, pp. 609–632.
- [7] Randell, D., Feld, G., Ewans, K., and Jonathan, P., 2015. “Distributions of return values for the ocean wave characteristics in the South China Sea using directional-seasonal extreme value analysis”. *Environmetrics*, **26**, pp. 442–450.
- [8] Vanem, E., Fazerer-Ferradosa, T., Rosa-Santos, P., and Taveira-Pinto, F., 2019. “Statistical description and modelling of extreme ocean wave conditions”. *Proceedings of the Institution of Civil Engineers - Maritime Engineering*, **172**, pp. 124–132.
- [9] Mackay, E., Haselsteiner, A. F., Coe, R. G., and Manuel, L., 2021. “A second benchmarking exercise on estimating extreme environmental conditions: Methodology & baseline results”. In Proc. 40th International Conference on Ocean, Offshore and Arctic Engineering (OMAE 2021), American Society of Mechanical Engineers (ASME).
- [10] Haselsteiner, A. F., Coe, R. G., Manuel, L., Chai, W., Leira, B., Clarindo, G., Guedes Soares, C., Hannesdóttir, Á., Dimitrov, N., Sander, A., Ohlendorf, J.-H., Thoben, K.-D., de Hauteclocque, G., Mackay, E., Jonathan, P., Qiao, C., Myers, A., Rode, A., Hildebrandt, A., Schmidt, B., Vanem, E., and Huseby, A. B., 2021. “A benchmarking exercise for environmental contours”. *Ocean Engineering*, **236**, p. 109504.
- [11] Mackay, E., de Hauteclocque, G., Vanem, E., and Jonathan, P., 2021. “The effect of serial correlation in environmental conditions on estimates of extreme events”. *Ocean Engineering*, **242**, p. 110092.
- [12] Coles, S., 2001. *An Introduction to Statistical Modeling of Extreme Values*. Springer-Verlag.
- [13] Monbet, V., Ailliot, P., and Prevesto, M., 2007. “Survey of stochastic models for wind and sea state time series”. *Probabilistic Engineering Mechanics*, **22**, pp. 113 – 126.
- [14] Bibby, B. M., Skovgaard, I. M., and Sørensen, M., 2005. “Diffusion-type models with given marginal distribution and autocorrelation function”. *Bernoulli*, **11**(2), pp. 191–220.
- [15] Bensoussan, A., and Brouste, A., 2018. “Marginal Weibull diffusion model for wind speed modeling and short-term forecasting”. In *Renewable Energy: Forecasting and Risk Management*, P. Drobinski, M. Mougeot, D. Picard, R. Plougonven, and P. Tankov, eds., Vol. 254 of *Springer Proceedings in Mathematics & Statistics*. Springer Nature, Switzerland, pp. 3–22.
- [16] Sim, C.-H., 1986. “Simulation of weibull and gamma autoregressive stationary process”. *Communications in Statistics - Simulation and Computation*, **15**(4), pp. 1141–1146.
- [17] Kaur, S., and Rakshit, M., 2019. “Gaussian and non-Gaussian autoregressive time series models with rainfall data”. *International Journal of Engineering and Advanced Technology*, **9**(1), pp. 6699–6704.
- [18] Papalexiou, S. M., 2018. “Unified theory for stochastic modelling of hydroclimatic processes: Preserving marginal distributions, correlation structures, and intermittency”. *Advances in Water Resources*, **115**, pp. 234–252.
- [19] Papalexiou, S. M., Markonis, Y., Lombardo, F., AghaKouchak, A., and Foufoula-Georgiou, E., 2018. “Precise temporal disaggregation preserving marginals and correlations (DiPMaC) for stationary and nonstationary processes”. *Water Resources Research*, **54**, pp. 7435–7458.
- [20] Carpena, P., Bernaola-Galván, P. A., Gómez-Extremera, M., and Coronado, A. V., 2020. “Transforming Gaussian correlations: Applications to generating long-range power-law correlated time series with arbitrary distribution”. *Chaos*, **30**, p. 083140.
- [21] DNV, 2021. *Environmental Conditions and Environmental Loads*, september 2019 ed. DNV. DNV-RP-C205.
- [22] Vanem, E., 2015. “Uncertainties in extreme value modeling of wave data in a climate change perspective”. *Journal of Ocean Engineering and Marine Energy*, **1**, pp. 339–359.
- [23] Papalexiou, S. M., Serinaldi, F., and Porcu, E., 2021. “Advancing space-time simulation of random fields: From storms to cyclones and beyond”. *Water Resources Research*, **57**, p. e2020WR029466.
- [24] Stefanakos, C. N., and Vanem, E., 2018. “Nonstationary fuzzy forecasting of wind and wave climate in very long-term scales”. *Journal of Ocean Engineering and Science*, **3**, pp. 144–155.
- [25] Vanem, E., 2018. “A simple approach to account for seasonality in the description of extreme ocean environments”. *Marine Systems & Ocean Technology*, **13**, pp. 63–73.
- [26] Zanini, E., Eastoe, E., Jones, M. J., Randell, D., and Jonathan, P., 2020. “Flexible covariate representations for extremes”. *Environmetrics*, **31**, pp. e2624:1–20.
- [27] Davis, R. A., and Mikosch, T., 2009. “The extremogram: A correlogram for extreme events”. *Bernoulli*, **15**(4), pp. 977–1009.
- [28] Davis, R. A., Mikosch, T., and Cribben, I., 2012. “Towards estimating extremal serial dependence via the bootstrapped extremogram”. *Journal of Econometrics*, **170**, pp. 142–152.